Assembling filamentous phage occlude pIV channels

Denise K. Marciano, Marjorie Russel, and Sanford M. Simon*

The Rockefeller University, 1230 York Avenue, New York, NY 10021

Edited by Günter Blobel, The Rockefeller University, New York, NY, and approved June 5, 2001 (received for review April 6, 2001)

Filamentous phage f1 is exported from its *Escherichia coli* host without killing the bacterial cell. Phage-encoded protein pIV, which is required for phage assembly and secretion, forms large highly conductive channels in the outer membrane of *E. coli*. It has been proposed that the phage are extruded across the bacterial outer membrane through pIV channels. To test this prediction, we developed an *in vivo* assay by using a mutant pIV that functions in phage export but whose channel opens in the absence of phage extrusion. In *E. coli* lacking its native maltooligosacharride transporter LamB, this pIV variant allowed oligosaccharide transport across the outer membrane. This entry of oligosaccharide was decreased by phage production and still further decreased by production of phage that cannot be released from the cell surface. Thus, exiting phage block the pIV-dependent entry of oligosaccharide, suggesting that phage occupy the lumen of pIV channels. This study provides the first evidence, to our knowledge, for viral exit through a large aqueous channel.

Filamentous phage comprise a large family of bacterial viruses that infect a variety of Gram-negative bacteria. They are rod-shaped particles ≈65 Å in diameter and ≈1 μm in length. Unlike most bacterial viruses, which are assembled in the cytoplasm and released by cell lysis, filamentous phage are coordinately exported as they are assembled at the cell surface in a secretory process that leaves the cells fully viable (1). The five structural proteins of the virus are anchored in the inner membrane before their incorporation into the phage particle (2), and the phage genome is present in the cytoplasm. As assembly begins, the phage genome traverses the inner and outer membranes, picking up two minor coat proteins, pVII and pIX, at the leading tip (3) and a helical array of major coat protein subunits (pVIII) along its length. When the entire DNA molecule has been coated and extruded, two other minor proteins, pIII and pVI, are added to the end of the virion (3). pIII and pVI are necessary to release the phage from the cell; in their absence, very long phage that contain multiple unit-length phage genomes are produced and remain attached to the cell surface (4, 5).

Three phage proteins that are not part of the mature virus are required for phage assembly and export: pI and pXI in the inner membrane (6–8) and pIV in the outer membrane (9). pIV shares significant sequence homology with outer membrane components of specialized types II and III protein secretion systems present in diverse species of Gram-negative bacteria. pIV and its homologs are termed secretins and constitute the only shared factor among the transport systems. As with filamentous phage assembly, these systems mediate translocation of macromolecules across the outer membrane. The exported macromolecules include type IV pili, degradative enzymes, and toxins, as well as protein kinases and phosphatases (10). The biological similarity of the bacterial and phage secretins is best illustrated by the *Vibrio cholerae* secretin EpsD. EpsD serves double duty for both secretion of cholera toxin by a type II secretion system and assembly and export of the filamentous phage, CTXϕ (11), which lacks gene IV. Further underscoring the relatedness of the two processes, the cholera toxin genes are carried on the CTXϕ genome (12).

Secretins are believed to serve as the conduits through which these large substrates travel across the outer membrane (1). This idea is based on observations that secretins are required for transport, form multimeric ring-like structures (13–16), and form ion-conducting channels when reconstituted in planar lipid bilayers (16–18). Our initial attempts to more directly test whether the channels formed by the secretin pIV are the conduits for the exported phage were inconclusive. We were unable to either visualize phage particles emerging from the central channel of pIV multimers purified from phage-producing cells or to modulate the conductance of reconstituted pIV channels by the addition of phage (unpublished data). Likewise, addition of pululanase did not affect the reconstituted PulD secretin (18).

The filamentous phage system is particularly well suited for testing the "channel-export" hypothesis *in vivo* for several reasons. The export secretin pIV forms distinctive large aqueous channels in planar bilayers. Point mutations in pIV that increase the probability of the channel opening *in vitro* also increase the permeability *in vivo* (17). The substrate is very large; at 65 Å, the diameter of the phage is close to that of the lumen of the pIV channel (70 Å), as measured by scanning transmission electron microscopy and calculated from its conductance in lipid bilayers (13, 17). Moreover, the phage length is 150 times its diameter. Thus, if the phage passes through the pIV channel, it might occlude the channel for an appreciable interval. Furthermore, although the phage is normally released into the extracellular milieu, it is possible to manipulate the assembly pathway so that phage remain tethered to the cell. The length of tethered phage produced in the absence of the minor phage coat protein pIII increases with time (4). This result indicates that phage tethered to the cell surface remain competent for elongation and suggests that they continue to occupy the pIV channel. In this paper, we present an *in vivo* assay to quantify the transport of macromolecules through the pIV channels. The export of filamentous phage reduces the transport of other macromolecules through pIV, suggesting that filamentous phage travel through these large aqueous channels.

MICROBIOLOGY

Materials and Methods

Bacteria, Phages, and Plasmids. *Escherichia coli* K12 strain MC4100 is F$^-$ *ara*Δ139 *lac* U169 *rel*A *thi rps*L (19). JB3018.2 is MC4100 *malT*^{c} (20) and GG2 is MC4100 *malT*^{c} *lamB*::*tn10* (W. Boos, University of Konstanz, Konstanz, Germany). Because F-pili are required for f1 infection, J3018.2 and GG2 were made F$^+$ by mating, creating DKM1 (J3018.2 F$^+$) and DKM2 (GG2 F$^+$). The *malZ*::*specR* null mutation from TK 38 (W. Boos) was introduced by P1 transduction and selection for spectinomycin resistance to create DKM3 and DKM4, respectively. K1793, a supF derivative of K38 (HfrC) that contains pJARA112 and pJARA131 (21), was used to prepare R756 phage. K1712 (17) carrying pPMR129 was used to prepare R484.

Plasmid pPMR129 (22) contains f1 gene IV$^+$ inserted be-

This paper was submitted directly (Track II) to the PNAS office.

Abbreviations: IPTG, isopropyl-β-D-thiogalactopyranoside; PG6, *p*-nitrophenyl-α-D-maltohexaoside.

*To whom reprint requests should be addressed. E-mail: simon@mail.rockefeller.edu.

The publication costs of this article were defrayed in part by page charge payment. This article must therefore be hereby marked "*advertisement*" in accordance with 18 U.S.C. §1734 solely to indicate this fact.

tween the *Hin*dIII and *Bam*HI sites of the polylinker region of vector pGZ119HE (23), putting geneIV^+ under the control of the isopropyl-β-D-thiogalactopyranoside (IPTG)-inducible tac promoter. pGZ119HE carries *lac*I^q, a chloramphenicol resistance gene, and a ColD origin of replication, which is compatible with the ColE1 origin of pMalS. Plasmid $pPMR129^{S324G}$ encodes pIV^{S324G}, with an amino acid substitution at residue 324 (Ser→Gly), that is functional for phage assembly (1). pUMu103, referred to here as pMalS, is a multicopy plasmid containing *malS* under the control of the *malT*^{c} promoter and a *bla* gene, which confers ampicillin resistance (20). Plasmid pJARA112 is a pBR322 derivative that contains f1 gene III under the control of the psp promoter, and pJARA131 is a pGZ119HE derivative that contains the *pspFABCD* operon, which modulates gene III expression from JARA112 (21).

f1 filamentous phage used were R484 (IV^- phage) and R756 ($III^- IV^-$ phage). R484 has a complete deletion of gene IV (24). R756 was constructed by combining the gene III deletion of R760 (21) with the chain-terminating amber mutation in the gene IV signal sequence from R427 phage (24).

PG6 Hydrolysis Assay. The assay was performed as described by Freundlieb *et al.* (20), with minor modifications. Cultures were grown at 37°C in M9 salts with 0.2% dextrose/0.2% casamino acids/50 μg/ml of ampicillin/50 μg/ml of chloramphenicol. When cultures reached an OD_{595} ≈0.6, IPTG was added to various concentrations, and cultures were grown for an additional 2 h. The cells were centrifuged for 10 min at 3,000 × *g* at room temperature, washed in fresh M9 medium without IPTG, and resuspended in fresh M9 medium to an OD_{595} = 2.0 (1×10^9 cells/ml). For cell permeabilization, 1:20 volume of 0.1% SDS and chloroform was added, and the samples were vortexed vigorously and allowed to stand for 10 min. The chromogenic substrate *p*-nitrophenyl-α-D-maltohexaoside (PG6) (Biochemicka/Fluka) was added to the tubes to a final concentration of 2 mM, or as indicated. The tubes were rotated at room temperature. Aliquots (0.5 ml) of the reaction were removed at specified times, and trichloroacetic acid was added to a final concentration of 3% to stop the reaction. The tubes were vortexed and placed on ice for 10 min, then centrifuged at 13,000 × *g* for 7 min at 4°C. The supernatant (0.4 ml) was removed into 0.6 ml of 2.0 M Na_2CO_3, and the OD_{405} values were determined.

The assay was modified as follows for phage-infected cells. IPTG was added at OD_{595} = 0.25, and the cells were grown for an additional 1 h at 37°C, shaking to OD_{595} ≈0.7. The cells were left standing at 37°C for 5 min to allow F-pili to regenerate and then infected with phage at a multiplicity of infection of 100 for 10 min at 37°C. Cells were harvested [SS34, 7,000 rpm (6,000 × *g*), 10 min] and resuspended to an OD_{595} of 2.0 in fresh M9 medium without IPTG. PG6 was added, and the tubes were rotated at 25°C. Aliquots were removed at specified intervals and reactions stopped with trichloroacetic acid. The assay was conducted at 25°C to eliminate reinfection by newly produced phage, because F-pili disassemble at temperatures below 34°C (25).

Preparation of Periplasm. The periplasm was prepared according to the method of Neu and Heppel (26). A 3-ml culture (OD_{595} 2.0) was centrifuged for 10 min at 3,000 × *g* at 4°C. The supernatant was discarded, and the cells were resuspended to 0.4 volumes in 30 mM Tris·HCl (pH 8.0) and 20% (wt/vol) sucrose. Na^+EDTA (pH 8.0) was added to 1 mM, and the tubes were rotated at room temperature for 10 min. The cells were centrifuged again for 10 min at 3,000 × *g* at 4°C. The supernatant was discarded, and the cells were resuspended in 0.6-ml ice-cold 5 mM $CaCl_2$, rotated at 4°C for 10 min, and centrifuged as above. The supernatant, now 5×, was diluted with 1.25× M9 medium to 3 ml (1× M9 final concentration), so that the periplasmic and whole cell assays could be performed in comparable solutions. The PG6 assay was performed as described above.

SDS/PAGE and Western Blot Analysis. Cells were collected by centrifugation and lysed by heating in 2% SDS to 100°C for 5 min. Samples (0.01 OD_{595}) were separated on 10% acrylamide-SDS gels (27) and then transferred to Nitropure nitrocellulose (Micron Separations, Westboro, MA) for 50 min at 100 V in transfer buffer. Blots were probed with 1:20,000 anti-pIV antibody in PBS/0.5% Tween overnight. Blots were washed three times with PBS/0.5% Tween and then incubated with 1:20,000 horseradish peroxidase-conjugated anti-rabbit antibody (Sigma) for 45 min. Blots were washed three times, and the secondary antibody was detected by using Supersignal Chemiluminescent Substrate (Pierce). Blots were exposed to Kodak X-Omat AR film.

Electron Microscopy. Cells were infected with phage, washed, and incubated for 2 h at 25°C. Cells were adsorbed onto glow-discharged carbon-coated grids, negatively stained with uranyl acetate, and examined on a JEOL 100 CX electron microscope.

Results

To quantify the rate of transport of macromolecules across pIV channels, we took advantage of the existing maltose/maltooligosaccharide transport system in *E. coli* (28). Transport of maltooligosaccharides across the bacterial outer membrane normally requires the maltoporin LamB (29). Once in the periplasm, short maltooligosaccharides are transported into the cytoplasm, where they are subsequently metabolized. Only maltooligosaccharides with six or fewer glucose residues can be transported into the cytoplasm; longer chains are first degraded by a periplasmic α-amylase, MalS (30, 31). Maltooligosaccharide transport through LamB has been quantified with a chromogenic analog of maltohexaose, PG6, which is hydrolyzed by MalS to maltohexaose and *p*-nitrophenol (20), a yellow compound whose concentration can be determined by measuring its absorbance at OD_{405} nm. When MalS is in excess such that PG6 is rapidly hydrolyzed on entry into the periplasm, the rate of PG6 hydrolysis is a quantitative measure of its permeation through LamB (20).

Our previous studies used pIV with a point mutation that changes Ser^{324} to Gly (pIV^{S324G}). This mutation, which is fully functional for phage export, produces a pIV channel that opens more frequently and facilitates bacterial growth on maltohexaose (17). In *E. coli* strains that lack LamB, we tested whether the rate at which PG6 was hydrolyzed could be used as an assay for transport through pIV^{S324G} (see Fig. 1). To optimize this assay, hydrolysis of PG6 should occur in the periplasm, and the transport of PG6 across the outer membrane should limit the rate of hydrolysis by MalS. Thus it was necessary to demonstrate that hydrolysis of PG6 was caused by neither cytoplasmic enzymes nor enzymes released from the cell and that the rate of hydrolysis was limited by the amount of pIV^{S324G}.

The rate of PG6 hydrolysis was measured in whole cells that contained periplasmic MalS expressed from a multicopy plasmid under control of the constitutive malT^c promoter. (Without this plasmid, levels of MalS produced from the chromosomal gene were insufficient to hydrolyze PG6 above background levels.) The cells contained either LamB, expressed at normal levels from the chromosomal gene, or wild-type pIV or pIV^{S324G}, expressed from a plasmid regulated by an IPTG-inducible promoter. The rate of cell growth, as assayed by OD_{595} and colony-forming units, was the same in all cultures, whether IPTG was present or not (data not shown). Equivalent numbers of cells were compared for a given experiment.

Cells containing mutant pIV^{S324G} (Fig. 2, open circles) showed a greatly increased rate of PG6 hydrolysis compared with

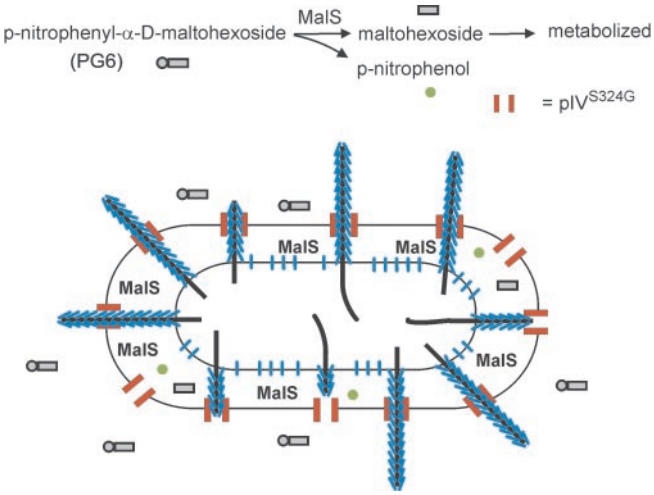

Fig. 1. Schematic of PG6 transport assay. When attached to maltohexaoside, the chromophore moiety of PG6, *p*-nitrophenol, is quenched; after hydrolysis by the periplasmic MalS, free *p*-nitrophenol absorbs at 405 nm. Absorbance by the chromophore (shown in green) reports hydrolysis of PG6 by the periplasmic MalS and indicates that PG6 had gained entry to the periplasm. Nascent phage assembling at pIV (red) are shown covered with their coat protein (blue).

uninduced cells (filled circles) or with the isogenic strain encoding pIV^{+} (open triangles, +IPTG), despite similar amounts of pIV and pIV ^{S324G} (Fig. 3*B*; compare lanes 5 and 7). Thus, pIV^{S324G}, unlike wild-type pIV, increases membrane permeability to PG6. Cells containing LamB hydrolyzed PG6 at a rate that was independent of IPTG (open/filled squares are +/−IPTG), as expected. Somewhat surprisingly, in cells producing LamB, PG6 was hydrolyzed more slowly than in cells producing pIV^{S324G}. This is likely due to slower rates of permeation per molecule, because LamB was much more abundant than pIV (data not shown).

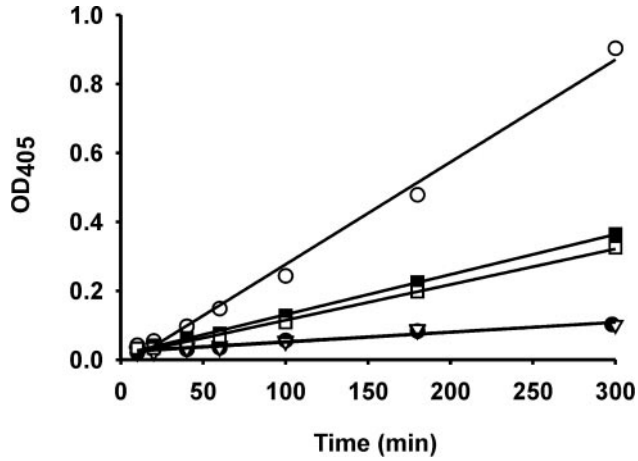

Fig. 2. PG6 hydrolysis by intact cells containing LamB, pIV^{+}, or pIV^{S324G}. DKM1 cells (*lamB*$^{+}$) with pMalS and empty vector and DKM2 cells (*lamB*$^{-}$) with pMalS and either the pIV^{+} or pIV^{S324G} plasmid were grown to OD_{595} 0.6 in M9 medium. Cells were incubated for an additional 2 h in the absence (filled symbols) or presence (open symbols) of 1 mM IPTG. The cultures were washed to remove IPTG and resuspended at OD_{595} 2.0 in medium containing 2 mM PG6. The cultures were sampled at the times indicated, and the OD_{405} was determined as described in *Materials and Methods*. LamB^{+}, no pIV (squares); no LamB, pIV^{+} (inverted triangles); no LamB, pIV^{S324G} (circles). One of three representative experiments is shown.

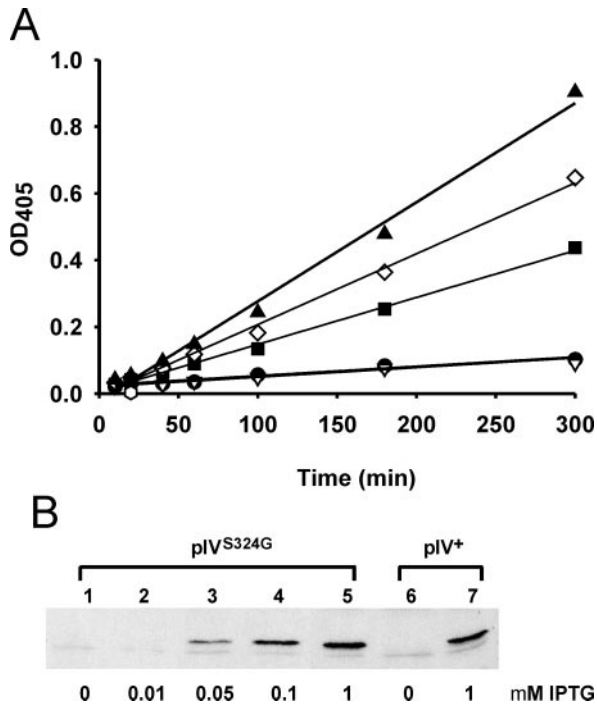

Fig. 3. PG6 hydrolysis with varying pIV^{S324G} levels. (*A*) DKM2 cells with plasmids encoding MalS and pIV^{S324G} were grown in the presence of 0 μM IPTG (circles)/10 μM IPTG (inverted triangles)/50 μM IPTG (squares)/100 μM IPTG (diamonds) or 1 mM IPTG (triangles) for 2 h before withdrawal of IPTG and addition of 2 mM PG6. The cultures were sampled at the times indicated, and the OD_{405} was determined as described in *Materials and Methods*. (*B*) Equivalent densities of cells grown for 2 h with IPTG at the indicated concentration were analyzed by Western blot as described in *Materials and Methods*. One of three representative experiments is shown.

We next tested whether the amount of pIV^{S324G} was rate-limiting for PG6 hydrolysis. Cells were grown with IPTG at various concentrations to induce different amounts of pIV^{S324G}, inducer was withdrawn, and PG6 hydrolysis and pIV amounts were measured (Fig. 3). Induction with 10 μM IPTG (inverted triangle) did not increase PG6 hydrolysis over baseline (circle), and no pIV was detected. Higher concentrations resulted in successively increased rates of hydrolysis (Fig. 3*A*) and amounts of pIV (Fig. 3*B*). The results demonstrate that the rate of PG6 hydrolysis is responsive to the amount of pIV, even after a 2-h induction with 1 mM IPTG (Fig. 3*B*, filled triangle). The constant rate of hydrolysis shows that after removal of IPTG there was no net additional production of pIV; additional pIV production would have increased rate of hydrolysis during the assay.

To test whether pIV affected the levels of MalS, the rate of PG6 hydrolysis was measured both in both permeabilized and whole cells (with the outer membrane intact) (Fig. 4). For these experiments, we used a *malZ*$^{-}$ strain lacking the cytoplasmic enzyme MalZ, which can also hydrolyze PG6. All cells with a MalS plasmid (Fig. 4*A*, lanes 2–6) had similar rates of PG6 hydrolysis when they were permeabilized, regardless of whether LamB, pIV, or neither protein was present. [This is 20-fold higher than MalS activity in a strain carrying only the chromosomal gene (Fig. 4*A*, lane 1)]. Comparable results were obtained with isolated periplasmic preparations of the equivalent *malZ*$^{+}$ strains (data not shown). The relative effects of expressing outer-membrane proteins on PG6 hydrolysis in intact *malZ*$^{-}$ cells (Fig. 4*B*) were equivalent to those in *malZ*$^{+}$ cells (Fig. 2): PG6 hydrolysis was greatly enhanced by pIV^{S324G}, LamB moderately increased the rate, and pIV^{+} did not increase it above

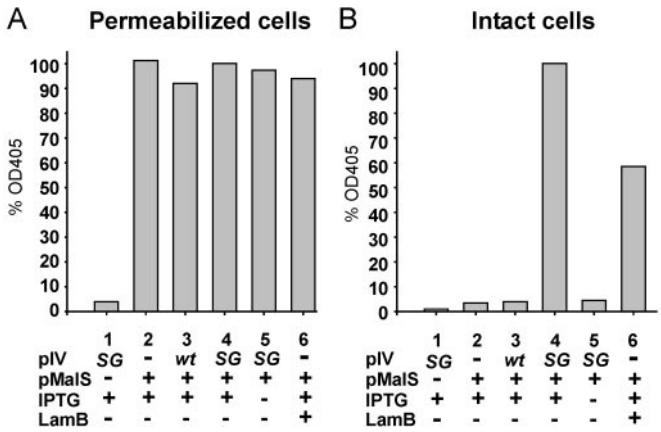

Fig. 4. PG6 hydrolysis in permeabilized or intact cells. Cells lacking MalZ (DKM3 and DKM4) were grown in the absence or presence of 1 mM IPTG for 2 h, rinsed, resuspended in (*A*) permeabilization buffer or (*B*) fresh medium, incubated with 2 mM PG6 for 1 h, and assayed as described in *Materials and Methods*. As indicated below the figure, the cells contained plasmids specifying pIV^{+} (wt), pIV^{S324G} (SG), or no pIV (−), the pMalS plasmid (+), or only the chromosomal *malS* gene (−), and were either *lamB*$^{-}$ (−) or *lamB*$^{+}$ (+). The PG6 hydrolysis values are expressed relative to lane 4. One of two representative experiments is shown.

background levels. Thus, cytoplasmic MalZ does not contribute to PG6 hydrolysis by intact cells. These results with permeabilized cells demonstrate that pMalS-containing strains have similar levels of MalS activity. Thus, differences in the rates of PG6 hydrolysis in intact cells are likely a consequence of differences in the accessibility of MalS to its PG6 substrate. There was little (<4%) MalS activity in the culture supernatants when cells were removed by centrifugation after incubation with IPTG (data not shown), which indicates that PG6 hydrolysis occurs in the periplasm.

The MalS activity of isolated periplasmic preparations (Fig. 5) saturated at much lower concentrations of PG6 (≈0.075 mM, inverted triangles) than in intact cells (>1 mM, circles). In this experiment, cells were induced for 2 h with 1 mM IPTG. Thus at PG6 concentrations below 1 mM, PG6 hydrolysis in intact cells

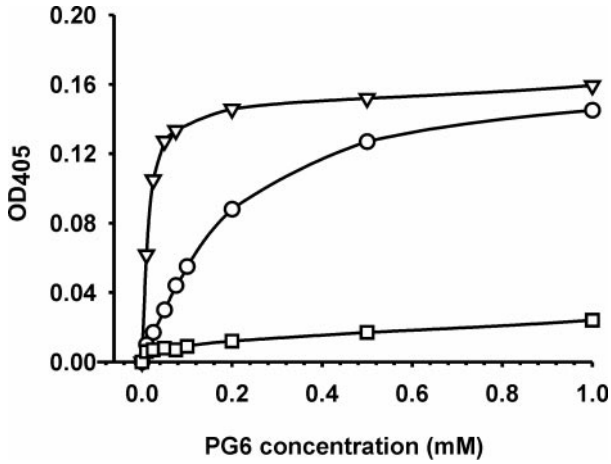

Fig. 5. PG6 hydrolysis as a function of PG6 concentration. DKM2 cells containing the pMalS and pIV^{S324G} plasmids were induced for 2 h with 1 mM IPTG, washed, and PG6 hydrolysis was assayed in intact cells (circles), the periplasmic fraction (inverted triangles) and intact cells not treated with IPTG (squares), as described in *Materials and Methods*. One of four representative experiments is shown.

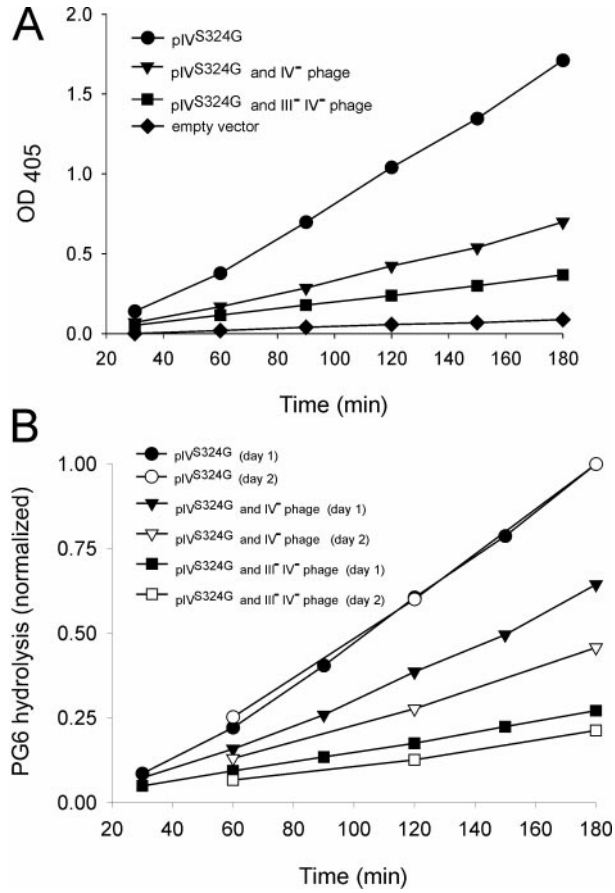

Fig. 6. PG6 hydrolysis in phage-infected cells. DKM4 cells containing pMalS and either pIV^{S324G} or the empty vector were grown with 1 mM IPTG for 1 h, infected with phage for 10 min, washed, and suspended in fresh medium that lacked IPTG. One portion of each culture was incubated with 2 mM PG6 and assayed at the times indicated, whereas another was permeabilized after 90 min and then incubated with PG6 to determine total MalS activity. (*A*) PG6 hydrolysis in pIV^{S324G}-containing uninfected cells (circles); IV^{-} phage-infected cells (inverted triangles); III^{-} IV^{-} phage-infected cells (squares); or uninfected cells that lacked pIV (diamonds). Each point is the average of two samples. (*B*) To facilitate comparison of experiments from different days, the data from *A* were normalized to total MalS. Uninfected cells (circles); cells infected with IV^{-} phage (inverted triangles); cells infected with III^{-} IV^{-} phage (squares). The results from 2 separate days are shown (equivalent results were seen in all experiments on 6 separate days).

is not limited by saturation of MalS; rather, it is limited by diffusion across the membrane.

These experiments (Figs. 3–5) allowed us to select conditions in which PG6 hydrolysis is limited by pIV-mediated diffusion across the outer membrane. Thus, MalS activity could be used to quantify transport through pIV^{S324G} channels. Together, the results show: (*i*) the amount of pIV remains constant during the experiment; (*ii*) MalS is not released from the cells; (*iii*) strains with pMalS have similar levels of MalS activity; and (*iv*) PG6 hydrolysis is limited by pIV^{S324G}-mediated diffusion across the outer membrane (and not by saturation of MalS) if the amount of pIV or PG6 is limited.

To test the hypothesis that phage are transported through pIV channels, we asked whether phage export decreased the pIV^{S324G}-mediated entry of PG6 entry into cells. A culture was induced to produce pIV^{S324G} for 1 h, and a portion was infected with phage for 10 min and then washed to remove IPTG and unadsorbed phage. PG6 was added and hydrolysis assayed at different times (Fig. 6*A*). The rate of PG6 hydrolysis was

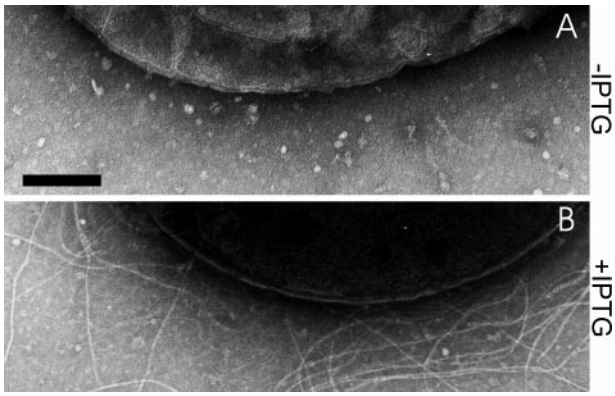

Fig. 7. Electron micrographs of cells infected with III$^-$ IV$^-$ phage. DKM4 cells containing the pMalS and pIV^{S324G} plasmids were grown (*A*) without or (*B*) with 1 mM IPTG for 2 h, infected with III$^-$ IV$^-$ phage, and washed before sampling for microscopy. (Scale bar = 200 nm.)

significantly slower in cells infected with IV$^-$ phage (triangles) than the rate in uninfected cells (circles). However, the rate of PG6 hydrolysis was still greater than control cells that carried the parental vector that lacked pIV (diamonds).

The decrease in PG6 hydrolysis could depend on how much time phage spend traversing open pIV^{S324G} channels during assembly and secretion. This hypothesis was tested by infecting cells with III$^-$ IV$^-$ phage that make neither pIV nor pIII. In the absence of pIII, phage particles are assembled and exported across the outer membrane, but they remain attached to the cell surface (4). The number of phage exported (in phage genomes) is similar to that in wild-type infected cells, and the physiology of the infected cells is unchanged. The attached phage are multiple lengths of the wild type and carry multiple copies of the phage DNA (4). That attached phage remain competent for further elongation indicates they are still engaged by the assembly machinery.

Electron microscopy on samples of *E. coli* infected with III$^-$ IV$^-$ phage confirmed that phage were produced and that they remained cell-associated under our experimental conditions. When pIV^{S324G} was present, numerous filamentous structures were associated with the bacteria (Fig. 7*B*), and virtually all were in close proximity to the cells. In contrast, it was difficult to find filaments in infected cells that lacked pIV^{S324G} (Fig. 7*A*); the few that remained most likely represent residual input phage.

Cells infected with III$^-$ IV$^-$ phage (Fig. 6*A*, squares) hydrolyzed PG6 at a rate that was still slower than the cells infected with the IV$^-$ phage (triangles). To facilitate comparison of the results from different days, in each experiment the rate of MalS hydrolysis in intact cells was normalized to the total MalS in a parallel aliquot of permeabilized cells. The results from 2 separate days (filled and open symbols) are plotted (Fig. 6*B*) for pIV^{S324G}-containing uninfected cells (circles), cells infected with IV$^-$ phage (triangles), and cells infected with III$^-$ IV$^-$ phage (squares). These experiments were repeated with variations in IPTG (50 μM to 1 mM) and PG6 (0.2, 0.5, and 2 mM) concentration. The results from all experiments (n = 7) were equivalent and preserved the relative ratios in the rates of PG6 hydrolysis (data not shown). Cells that lacked pIV^{S324G} did not show increased permeability to PG6 when infected with IV$^-$ or III$^-$ IV$^-$ phage compared with their uninfected counterpart (data not shown), indicating that other phage proteins and/or their interactions with bacterial proteins do not make the outer membrane leaky to PG6.

Discussion

The location and ultrastructural and biophysical properties of pIV suggest that it serves as a conduit for the assembling phage. However, this idea had not previously been tested for pIV or for any of the bacterial secretins. In this study, we quantified macromolecular transport through pIV channels *in vivo* and then assessed whether phage production could block transport. The assay relied on a periplasmic amylase, MalS, to hydrolyze a chromogenic maltooligosacharride, PG6. In wild-type *E. coli*, the maltoporin LamB transports PG6 across the outer membrane into the periplasm, where it is subsequently hydrolyzed by MalS (20). In the absence of LamB, transport (and thus hydrolysis) of PG6 does not occur. Wild-type pIV was unable to substitute for LamB to facilitate PG6 transport, which is consistent with our previous results that pIV$^+$-containing cells cannot use maltohexaose as a carbon source and that pIV$^+$ channels remain closed in bilayers, except at very high voltages (17). However, a mutant pIV (pIV^{S324G}) that is functional for phage assembly and opens at moderate voltages was able to efficiently substitute for LamB, thus mediating diffusion of PG6 into the periplasm.

Assay conditions were established to maximize the rate of PG6 hydrolysis while at the same time ensuring that PG6 diffusion through pIV channels remained rate-limiting for its hydrolysis. The rate of PG6 transport through pIV^{S324G} channels was significantly decreased in cells producing phage that were released from the cell, and it was severely reduced when the produced phage remained attached to the cell surface. That PG6 transport decreased substantially in cells producing tethered phage compared with those producing released phage indicates that phage infection *per se* cannot account for the decrease in PG6 transport. That is, the changes in cell physiology or structure caused by phage infection were not responsible for the reduction in PG6 hydrolysis. Furthermore, the infected cells were derived from a single culture and thus contained the same amounts of MalS and pIV^{S324G}. The only difference between them was the presence or absence of pIII, the protein that allows tethered phage to be released from the cell. pIII itself does not affect the permeability of infected cells to PG6, because infected cells lacking pIV^{S324G} showed similar low levels of PG6 transport, whether or not pIII was present (data not shown).

Cells producing tethered phage had a substantial reduction in PG6 transport compared with uninfected cells. The reduction was somewhat greater than we had expected. However, it is consistent with the observation that assembly and export of f1 filamentous phage does not compromise the integrity of the host bacterium. Therefore, a reasonably close seal must exist between pIV and the extruding phage. The rate of PG6 hydrolysis in cells producing phage tethered to the cell surface was somewhat higher than the background measured in cells lacking pIV^{S324G}, thus the blockade of PG6 transport by phage was not 100%. Potentially, extruding phage may not completely occlude the pIV^{S324G} channels, allowing some diffusion of PG6 to occur even when the phage is trapped in the lumen. This is consistent with the ability to incorporate fusion proteins into the coat of extruding phage.

These observations indicate that export of phage particles reduces import of a large maltooligosaccharide through pIV^{S324G} channels. One inference is that the phage exit through the lumen of the pIV channels, as diagrammed in Fig. 1. Given that pIV is similar in sequence, structure, and secretory function to types II and III secretins, we postulate that these bacterial secretins also function as conduits through a similar mechanism.

We thank Winfried Boos for strains and helpful advice. We are grateful to Michael Shiloh, Peter Model, and Mark Goulian for numerous discussions and critical reading of the manuscript. We thank Eleana Sphicas for electron microscopy. This work was supported by National Institutes of Health (NIH) Medical Scientist Training Program Grant GM07739 (to D.K.M.), National Science Foundation Grant MCB93-16625 (to M.R.), NIH Grant R01EY12346, and the Keck Foundation (S.M.S.).

1. Russel, M., Linderoth, N. A. & Sali, A. (1997) *Gene* **192,** 23–32.
2. Endemann, H. & Model, P. (1995) *J. Mol. Biol.* **250,** 496–506.
3. Lopez, J. & Webster, R. E. (1983) *Virology* **127,** 177–193.
4. Rakonjac, J. & Model, P. (1998) *J. Mol. Biol.* **282,** 25–41.
5. Rakonjac, J., Feng, J. & Model, P. (1999) *J. Mol. Biol.* **289,** 1253–1265.
6. Haigh, N. G. & Webster, R. E. (1999) *J. Mol. Biol.* **293,** 1017–1027.
7. Feng, J. N., Model, P. & Russel, M. (1999) *Mol. Microbiol.* **34,** 745–755.
8. Rapoza, M. P. & Webster, R. E. (1995) *J. Mol. Biol.* **248,** 627–638.
9. Russel, M. (1995) *Trends Microbiol.* **3,** 223–228.
10. Thanassi, D. G. & Hultgren, S. J. (2000) *Curr. Opin. Cell Biol.* **12,** 420–430.
11. Davis, B. M., Lawson, E. H., Sandkvist, M., Ali, A., Sozhamannan, S. & Waldor, M. K. (2000) *Science* **288,** 333–335.
12. Waldor, M. K. & Mekalanos, J. J. (1996) *Science* **272,** 1910–1914.
13. Linderoth, N. A., Simon, M. N. & Russel, M. (1997) *Science* **278,** 1635–1638.
14. Koster, M., Bitter, W., De Cock, H., Allaoui, A., Cornelis, G. R. & Tommassen, J. (1997) *Mol. Microbiol.* **26,** 789–797.
15. Crago, A. M. & Koronakis, V. (1998) *Mol. Microbiol.* **30,** 47–56.
16. Brok, R., Van Gelder, P., Winterhalter, M., Ziese, U., Koster, A. J., De Cock, H., Koster, M., Tommassen, J. & Bitter, W. (1999) *J. Mol. Biol.* **294,** 1169–1179.
17. Marciano, D. K., Russel, M. & Simon, S. M. (1999) *Science* **284,** 1516–1519.
18. Nouwen, N., Ranson, N., Saibil, H., Wolpensinger, B., Engel, A., Ghazi, A. & Pugsley, A. P. (1999) *Proc. Natl. Acad. Sci. USA* **96,** 8173–8177.
19. Casadaban, M. J. & Cohen, S. N. (1979) *Proc. Natl. Acad. Sci. USA* **76,** 4530–4533.
20. Freundlieb, S., Ehmann, U. & Boos, W. (1988) *J. Biol. Chem.* **263,** 314–320.
21. Rakonjac, J., Jovanovic, G. & Model, P. (1997) *Gene* **198,** 99–103.
22. Daefler, S., Russel, M. & Model, P. (1997) *J. Mol. Biol.* **266,** 978–992.
23. Lessl, M., Balzer, D., Lurz, R., Waters, V. L., Guiney, D. G. & Lanka, E. (1992) *J. Bacteriol.* **174,** 2493–2500.
24. Brissette, J. L. & Russel, M. (1990) *J. Mol. Biol.* **211,** 565–580.
25. Hoffmann-Berling, H. & Maze, R. (1964) *Virology* **22,** 305–313.
26. Neu, H. C. & Heppel, L. A. (1965) *J. Biol. Chem.* **240,** 3685–3692.
27. Laemmli, U. K. (1970) *Nature (London)* **227,** 680–685.
28. Boos, W. & Shuman, H. (1998) *Microbiol. Mol. Biol. Rev.* **62,** 204–229.
29. Wandersman, C., Schwartz, M. & Ferenci, T. (1979) *J. Bacteriol.* **140,** 1–13.
30. Ferenci, T., Brass, J. & Boos, W. (1980) *Biochem. Soc. Trans.* **8,** 680–681.
31. Ferenci, T. (1980) *Eur. J. Biochem.* **108,** 631–636.